Estimating local modulus of elasticity in a beam from bending measurements: An overview

Friend K. Bechtel*
Chin S. Hsu
Timothy C. Hanshaw

Abstract

Bending modulus of elasticity measurements have been useful and profitable for decades in the sorting of dimension lumber for its structural quality. Bending and tensile strengths of lumber are known to be correlated with modulus of elasticity. Previous research indicates that knowledge of elasticity properties on shorter spans may improve the correlation with strength. However, for practical reasons, bending spans cannot be as short as the desired measurement resolution. It is expected, therefore, that the optimal estimation method of the present work will be applied in the machine stress rating (MSR) process for more accurate sorting of dimension lumber into MSR grades. We describe a method for estimating local modulus of elasticity along the length of a beam. A sequence of measurements from overlapping bending spans, such as those obtained in equipment for MSR lumber production, is processed using a new concept called "span function." The method is feasible in real-time, and the primary requirement for its implementation with high-speed, production-line equipment is additional software. Tests indicate that the method may be immediately applicable in reducing measurement noise in the MSR process, thereby improving grading accuracy. Further, it is likely that improved grading algorithms will be developed that make use of local elasticity properties. Because of the large throughput volume of modern MSR machinery, the profit increment from reduced measurement noise alone has the potential for funding the research into better grading algorithms.

Bending modulus of elasticity measurements have been useful and profitable for decades in the sorting of dimension lumber for its structural quality. Bending and tensile strengths of lumber are known to be correlated with modulus of elasticity. Previous research indicates that knowledge of elasticity properties on shorter spans may improve the correlation with strength. However, for practical reasons, bending spans cannot be as short as the desired measurement resolution. It is expected, therefore, that the optimal estimation method of the present work will be applied in the machine stress rating (MSR) process for more accurate sorting of dimension lumber into MSR grades.

Wood is a highly variable material, and there has been significant historical interest in better determination of local modulus of elasticity. Clearly, the assumption that local modulus of elasticity within a bending span is uniformly the same as measured modulus of elasticity from a bending measurement is made only because of the inability to obtain the local values from bending measurements. An early paper (Kass 1975) discussed some of the precision difficulties involved with bending measurements for short span lengths. Kass described method and laboratory equipment for determining bending values on various span lengths from 203 mm to 610 mm and was able to show evidence of a knot corresponding to minima for short spans that was not evident from longer span data. Other work has shown that measurements on shorter spans have provided better correlation with strength (Orosz 1976).

The authors are, respectively, Managing Member, Kierstat Systems LLC, Mead, WA (fbechtel@ieee.org); Professor (deceased) and Instructor, Electrical Engineering, Washington State Univ., Pullman, WA (thanshaw@eecs.wsu.edu). In part, this material is based upon work supported by the USDA under Grant No. 00-33610-8896. Any opinions, findings, and conclusions or recommendations expressed in this publication are those of the authors and do not necessarily reflect the views of the USDA.
This paper was received for publication in February 2006. Article No. 10160.
*Forest Products Society Member.

Forest Prod. J. 57(1/2):118-126.

Objectives

Our first objective is to use a sequence of overlapping bending modulus of elasticity measurements along the length of a beam and optimally estimate local modulus of elasticity for each increment in a subdivision of the beam length. Our second objective is to show how better resolution of local properties will be useful for better determination of structural quality of a beam. We think the work has commercial value and will improve the accuracy, and hence profitability, of the machine stress rating (MSR) process, which sorts dimension lumber into MSR grades.

Background

Modulus of elasticity and compliance

Before proceeding, we define more precisely the measured and local property functions. Almost all the literature involving bending measurements and the intrinsic material properties leading to these measurements has involved modulus of elasticity; but, our work uses compliance. From measured modulus of elasticity, we define measured compliance $C_m = 1/E_m$. Similarly, from local modulus of elasticity, we define local compliance $C = 1/E$. It is not that we prefer to use compliance over modulus of elasticity; rather, a derivation shows it is compliance that has a desired convolution relationship useful for our results.

The span function, a necessary concept

Span function is a weighting function that shows how each local compliance along the length of a beam contributes to a bending measurement of compliance. A platform scales analogy is helpful in explaining the span function concept. Suppose a line of people marches across the platform of a platform scales in single file. As one person steps off, another steps on so that for each measurement the total weight of 10 people is obtained. Now, if the totals are each divided by 10 to get a sequence of weighted averages, the result is analogous to our compliance measurements. In this case, the weighting function (span function) is uniform; that is, each person's weight contributes to the result independently of his position on the platform. Carrying the analogy further as related to the present work, the problem is to estimate each person's weight, i.e., the local weight, from the measurement sequence of weighted averages. For a bending span applied to a beam, the span function is *not* uniform, and each local compliance contributes differently to the measurement depending on its position along the span.

Review of previous work

The span function for a simply-supported, center-loaded bending span was derived by Bechtel (1985). **Figure 1** illustrates this span function for two different span lengths. The measured compliance function obtained from bending measurements along a beam was shown to be the mathematical convolution of the local compliance function and the span function. Because of the convolution theorem of mathematics, wherein, after taking Fourier transforms, the convolution of two functions becomes multiplication, it was natural to suggest obtaining the local function by division followed by an inverse Fourier transform operation. In the following, h refers to the span function, and $*$ indicates convolution. The convolution relationship is:

$$C_m = C * h \qquad [1]$$

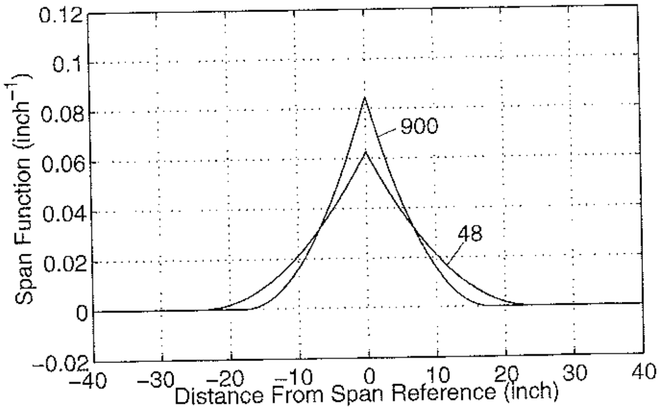

Figure 1. — Span functions for simply-supported, center-loaded bending spans of 1219 mm (48 inch) and 900 mm.

After converting convolution to multiplication by taking Fourier transforms, the relationship becomes:

$$\overline{C_m} = \overline{C} \cdot \overline{h} \qquad [2]$$

where the overbar indicates Fourier transform of the function beneath it, and $\cdot$ indicates multiplication. From [2], division gives:

$$\overline{C} = \frac{\overline{C_m}}{\overline{h}} \qquad [3]$$

It seems then that taking the inverse transform of the quotient in [3] should give the desired local compliance C. However, the measurement of C_m is typically noisy, particular at high frequencies. This noise and the fact that the Fourier transform of h in the denominator of [3] is very small at high frequencies renders the inverse transform of the ratio in [3] useless due to its high frequency noise.

A computationally intensive method was developed (Bechtel and Allen 1985) to reduce noise effects and was applied to flatwise bending measurements for one piece of Radiata Pine lumber with cross-section dimensions 38 mm by 89 mm (1.5 inch by 3.5 inch)[1]. The bending apparatus was an off-line tester modified to have a simply-supported, center-loaded bending span 1219 mm (48 inch) long. Compliance measurements were made every 19 mm (3/4 inch) as this wood beam was moved longitudinally relative to the bending apparatus. The result was a graph, presented here as **Figure 2**, which reveals two local minima in the local E function over a 300 mm (12 inch) segment where the measured E_m showed only one. These minima corresponded to two knots observed on the measured board.

The computational intensiveness of the method was discouraging. Also, there is a problem with end effects due to Gibb's phenomenon (Guillemin 1949) that must be dealt with when using the Fourier transform on a finite-length wood beam. While the result in **Figure 2** used the span function and measured data from a simply-supported, center-loaded bending span, Bechtel (1985) erroneously suggested applying the

[1] There is some inconsistency in our use of units. An effort has been made to convert to SI units where practical, but instances remain where existing data and graphs are expressed in English units. Where it seems useful, units in both systems are given in the text.

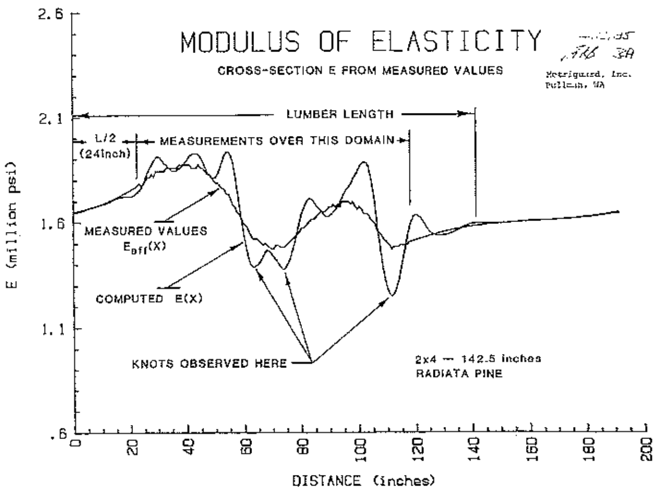

Figure 2. — Measured E_m *(=* E_{eff}*) from simply-supported, center-loaded bending span 48 inches long (Bechtel and Allen 1985). Computed local E used the measured* E_m *sequence, the span function* ***48*** *of* ***Figure 1****, and the Fourier transform method with a numerically intensive procedure to reduce noise. Local E clearly distinguishes two knots in a region of the beam where only one might be inferred from measured* E_m*.*

same span function to data from clamp-roller-supported spans used in high-speed production machinery.

Others (Foschi 1987, Lam et al. 1993, Pope and Matthews 1995) also applied the Fourier transform method to estimate local compliance values. These efforts used frequency truncation to reduce unwanted high frequency noise. Pope and Matthews concluded that the resulting local E was only marginally better than measured E_m for estimating bending strength. All of this work used a simply-supported, center-loaded span function. While frequency truncation is useful in reducing noise, it is a suboptimal, ad hoc approach to the problem.

Shear deflections and their local variations are not considered. We believe the effects due to shear are of second order in the proposed MSR lumber grading application because of the relatively large span-to-depth ratios used. However, shear effects may be important in other applications. In that case more involved derivations may be required.

Computing span function

We give a computational procedure for obtaining the span function for a bending span having a general system of support points. Graphs of span functions for several commonly used bending spans are presented. Acceleration forces at the supports are assumed negligible. Thus, the work is not directly applicable for some older production-line machines in cases where support point apparatus may translate as deflections change, e.g., in response to a constant load. This is not an issue for modern high-speed bending machinery using fixed supports or for off-line machinery where supports deflect slowly. The E-computer mentioned last in this section is treated as a special case.

For a given bending span arrangement of support points, basic beam theory (Higdon et al. 1960) allows measured compliance C_m to be obtained as a function of support deflections divided by a function of support forces. If the local compliance is constant, say $C = C_o$, the computed "measured" compliance C_m will equal the constant local value C_o.

We can also compute a measured compliance if the local compliance function is a constant plus an impulse of compliance. The impulse is a mathematical construct that has infinite height and zero width; but, it has area "b" known as the impulse weight. Think of this as a very short and very limber region of the beam at a specific point along the beam. A compliance impulse could be approximated by a sawkerf across the width and partway through the thickness of a wood beam. Suppose this beam is measured for bending compliance by a simply-supported, center-loaded bending span. It seems intuitively clear that the compliance impulse will have little effect on the measured compliance if it is near an end support of the bending span and maximum effect if it is in the middle of the span, and that the effect will decrease as the weight b of the impulse is decreased (e.g., depth and/or width of sawkerf is decreased). This made-up local compliance function consisting of a constant plus an impulse is used in the computation of span function.

The span function $h(x)$ is the difference between the measured compliance with impulse and the measured compliance without impulse, this difference being divided by the impulse weight b and taken to the limit as b approaches zero. The limiting operation can be written as a partial derivative so that the span function $h(x)$ is given by:

$$h(x) = \lim_{b \to 0} \left[\frac{C_m(b,x) - C_o}{b} \right] = \left. \frac{\partial C_m(b,x)}{\partial b} \right|_{b=0} \qquad [4]$$

where $C_m(b,x)$ is the measured compliance when the local compliance is the constant C_o plus an impulse of weight b at position x, and x is the impulse position relative to a bending span reference. Derivation of [**4**] and details of computing the span function for bending spans of interest are in the cited literature (Bechtel 2007, Bechtel et al. 2006). Generally, computation of the derivative involves performing the limiting operation in [**4**].

Span functions for specific useful bending span configurations

Simply-supported, center-loaded bending span

This commonly used arrangement has a span function that is zero outside the bending span and consists of two quadratic pieces within the span as shown in **Figure 1** for both 900 mm and 1219 mm (48 inch) spans. The span function labeled **48** in **Figure 1** was used to obtain the result in **Figure 2**.

Production-line machine

Referring to **Figure 3**, each bending section of one type of machine used to produce MSR lumber (back cover of this journal, Bechtel et al. 1996) uses support rollers **1** at seven support points $\{x_i\}_{i=1}^{7}$. Each measurement E_m is taken as proportional to the load seen on the support at x_4. As a beam **2** progresses through this system of supports, useful measurements begin when the leading end **7** engages just the first five supports as illustrated in **Figure 3**. Then, as it progresses further, it will engage the first six supports, then all seven, then the last six, and finally just the last five supports. Each of the five bending spans thus identified has a "central region" in common, namely the 1219 mm (48 inch) region between supports x_3 and x_5 in **Figure 3**. Each bending span has a different span function plotted in **Figure 4** and labeled in order **31**.

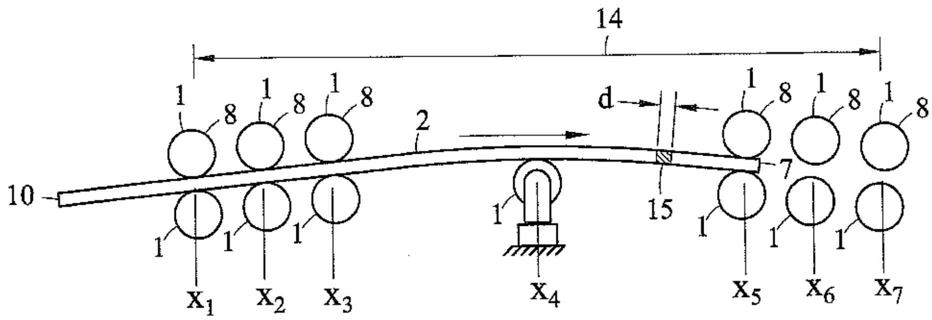

Figure 3. — A production-line configuration of seven support points at x_1 *through* x_7 *is illustrated. An increment* ***15*** *of the beam length subdivision is shown. The extent of the bending span* ***14*** *can change depending on how many supports are engaged; in the figure, the span extent* ***14*** *is inconsistently shown as though all seven supports were engaged, when in fact the beam* ***2*** *is engaging only the first five.*

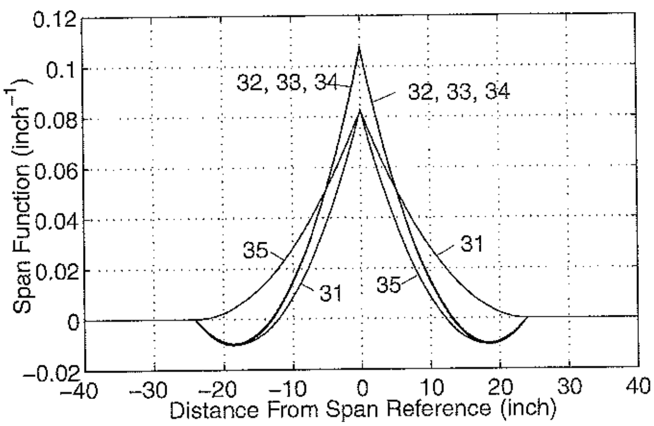

Figure 4. — Span functions for the five applicable bending spans of ***Figure 3*** *for beams longer than* $x_7 - x_1$ *= 2032 mm (80 inch). The sequence of 5, 6, 7, 6, and then 5 supports engaging the beam as the beam progresses through the system has respectively the span functions labeled* ***31, 32, 33, 34,*** *and* ***35****. The span functions for the 6 and 7-support cases are indistinguishable from one another on the scale of this graph. The 5-support span functions* ***31*** *and* ***35*** *are clearly different from the others and from each other.*

32, . . . , **35**, as a beam engages them while passing through. On the scale of the figure, the differences among the six and the seven support configurations **32**, **33**, and **34** cannot be seen. This sequence of span functions is valid under the assumption that the beam is longer than $x_7 - x_1$, i.e., 2032 mm (80 inch).

The example span functions of **Figure 4** are idealized versions and were computed with the assumption of rigid and perfectly aligned supports. Flexure of the supports and compression of wood fibers at the support points can be modeled and included in the computation of span functions as can deviations from perfect alignment. Generally, a lack of rigidity leads to a softening of span function shape. Instead of the span functions in **Figure 4** returning crisply to zero at plus and minus 610 mm (24 inch) from span center, the functions return more smoothly to zero outside the central region thereby increasing the extent of the domain where the span functions are nonzero. Differences not seen among the span functions labeled **32, 33,** and **34** in **Figure 4** are more pronounced if the supports are not completely rigid, and amplitudes of the span functions in the center of the central region are reduced. Misalignment of the supports in **Figure 3** also changes the span function shape and extent.

Bending proof load testers

In North America two different configurations are commonly used in bending proof load testers for off-line quality control of bending modulus of elasticity. **Figure 5** illustrates both configurations. Four equally spaced supports provide loading of a beam **2**. Equal forces are applied in one direction at the inner two supports with reaction forces in the opposite direction at the outer supports. In the first configuration, beam deflection is measured **54** as the average of the support deflections at the inner two supports. In the second configuration, deflection is measured **55** at span center, and it is necessary for span function computations to introduce a zero-force, center support between the inner two supports. Deflection at center span is measured at this center support, and a five support system is solved where the center support force is specified as zero. The span functions computed for these two configurations of proof testers are illustrated in **Figure 6**. Full details of these computations may be found elsewhere (Bechtel et al. 2006). From **Figure 6**, the span functions for these machine configurations are not identical even though bending moments in a tested beam are. Compliances in the center third of the bending span contribute equally to measured compliance in the first case, but not in the second. These differences may be important for specifying quality control procedures that determine whether a wood beam satisfies grade requirements.

Transverse vibration *E*-computer

The transverse vibration *E*-computer takes advantage of the differential equation modeling a transversely vibrating beam, simply supported at its ends, to relate the fundamental vibration frequency, beam weight, beam dimensions, distance between supports and beam modulus of elasticity. Measured E_m (or measured C_m) is computed from the other quantities in this relationship. In the model, local density and compliance are assumed uniform along the beam length. Our span function computation allows us to determine the effect of local compliance variations.

The *E*-computer span function is computed following the procedure of Equation [**4**] where a compliance test function with compliance impulse is introduced. The resulting span function is given by:

$$h(x) = \frac{1 - \cos(2\pi x/L)}{L}, \quad 0 \le x \le L \qquad [5]$$

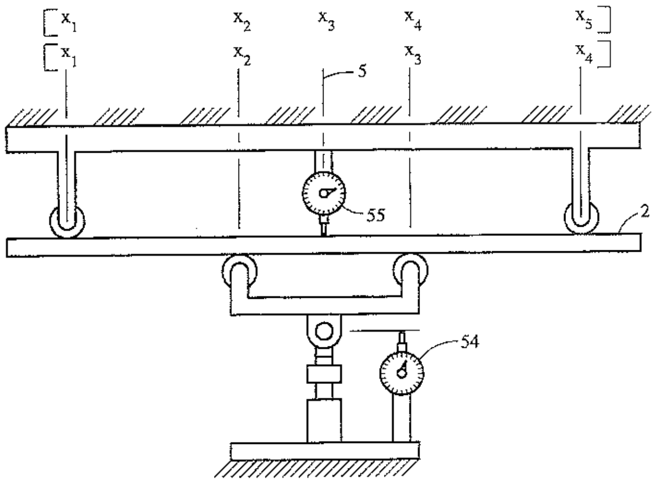

*Figure 5. — Mechanical schematic for two bending proof load testing configurations. The first measures deflection at **54** as the average of the loading support deflections. The second measures deflection **55** at span center. While induced moments in a tested beam **2** are identical, the span functions are different (see **Figure 6**).*

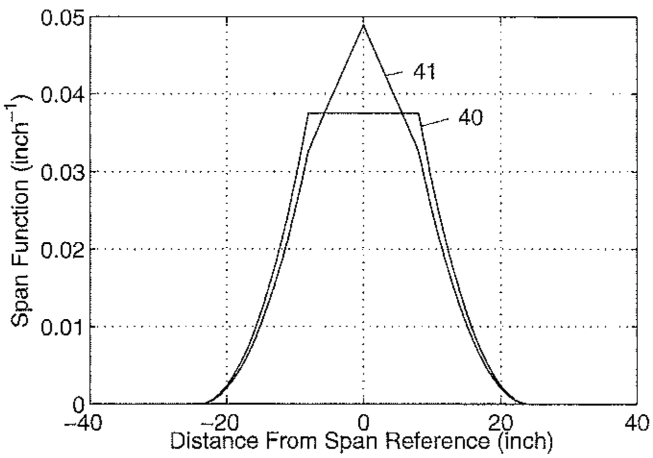

*Figure 6. — Span functions for the two configurations of **Figure 5**. Span function for deflection measurement **54** in **Figure 5** is shown as curve **40**. Span function for deflection measurement **55** in **Figure 5** is shown as curve **41**.*

where L is the distance between supports. The E-computer span function, illustrated in **Figure 7**, is a raised cosine function. This result is incomplete because it does not account for density variations within a beam, which affect the dynamics of the vibration. However, Equation [5] does answer the question sometimes raised with the E-computer method about the effects of local compliance variation along the length of a tested beam. The result is included to illustrate the generality of the method for computing span function.

Description of compliance measurements as a sample function from an ARMA random process

Refer now to the block diagram of **Figure 8** where **14** represents the extent of the bending span. First, consider just the upper part, the autoregressive (AR) part, of the block diagram involving the autoregression parameters $\{a_i\}_{i=1}^{p}$, which define the statistical structure among the local compliance values.

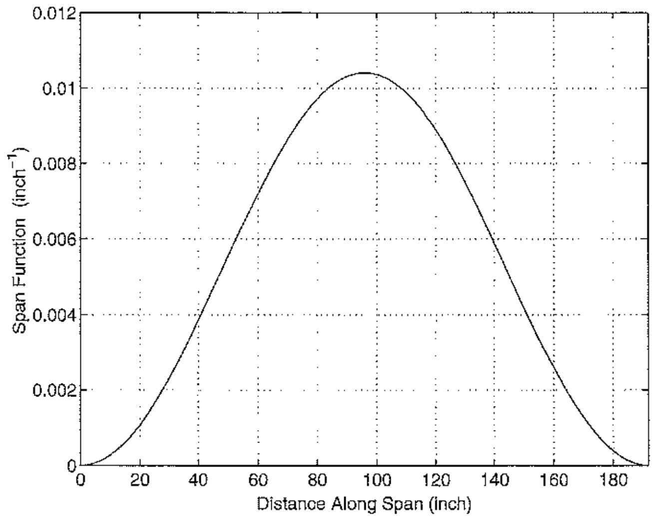

Figure 7. — Transverse vibration E-computer has a raised cosine span function.

The unknown local compliance values are given statistical structure to recognize and take advantage of the fact that they are correlated. For example, if the local compliance value were known for one length increment in a subdivision of the beam, then it is likely that the value in an adjacent length increment will be nearly the same.

Imagine that a beam is moving in steps indexed by k from left to right through the vertical center of the block diagram with the leading end starting off at the left of the diagram at **11**. The local compliance of the first increment of the beam is represented by a random number $u(k)$ at **11**. It goes through a delay (beam moves to the right by one step) and is fed back via (multiplied by) autoregression parameter a_1 and added (with a minus sign) to a random number $u(k + 1)$ to give the local compliance for the second increment of the beam at **11**. Both first and second increment compliances go through delays (denoted by blocks with z^{-1}) and are fed back via parameters a_2 and a_1 respectively and added to random number $u(k+2)$ to give the local compliance for the third increment of the beam at **11**; and so on. When the lead end of the beam gets to the right side of the block diagram, a set of p unknown local compliance values, represented by $\{s_i(k)\}_{i=1}^{p}$ and having the desired statistical structure, has been defined. The beam has just completed the bending span **14**, its lead end is ready to exit the span, and it is in position for modeling the first measured compliance.

From the span function at step k, a set of weights $\{h_i(k)\}_{i=1}^{p}$ summing to one is computed. The weights are areas under the span function over equal length increments in a regular subdivision of its domain. These increment lengths are equal to the increment lengths of the beam's subdivision. Consider the lower part, the moving average (MA) part, of the block diagram in **Figure 8**. The (unknown) local compliance values $s_i(k)$ are multiplied by the weights $h_i(k)$ in inverse order and the products summed along with measurement noise $v(k)$ to give the measured compliance $y(k)$ as a noisy weighted average of the local compliances. The dependence of the weights $h_i(k)$ on k indicates that the bending span and weights may change during the measurement process. Not only can the

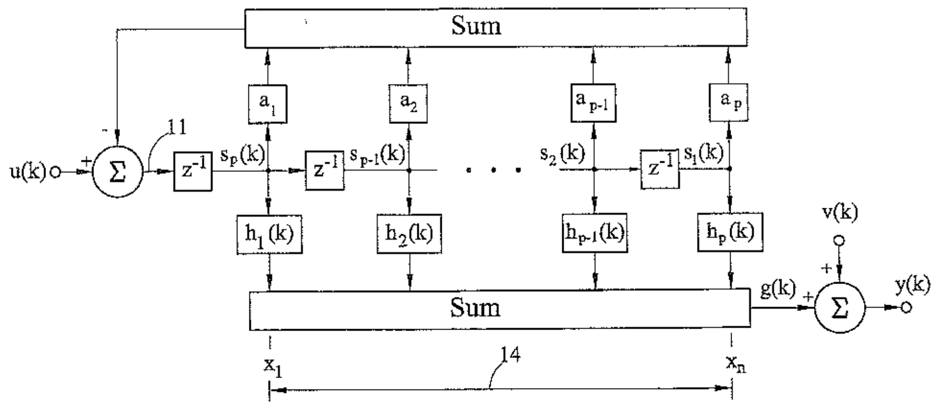

*Figure 8. — Block diagram of ARMA model for measured compliance C_m. A wood beam can be thought of as moving from left to right at the vertical center of the diagram, and the local compliances are in correspondence with the components $\{s_i(k)\}_{i=1}^{p}$ of a state vector at any measurement step k. The blocks labeled z^{-1} are delays. Autoregression parameters $\{a_i\}_{i=1}^{p}$ relate compliances along the beam, and the weights $\{h_i(k)\}_{i=1}^{p}$ are computed from the span function applicable at measurement step k. If the lead end of the beam is at the right of the diagram, then it has just completed the bending span **14**, and the first p local compliance values of the beam are in correspondence with the p state variables. At the next measurement step, when the beam has moved one increment to the right, local compliances 2 through p + 1 are in correspondence with the p state variables.*

weights change with k, but the number of them can change[2], which implies that the extent **14** of the bending span can change.

As the beam moves to the right, another (overlapping) set of local compliances is weighted to give the next measured compliance, all according to a discrete signal version of the convolution in Equation **[1]** (Oppenheim and Schafer 1989). The set of compliance measurements is a moving average (MA) of the local compliances. The autoregressive (AR) model for the local compliances followed by the moving average measurement allows the compliance measurement sequence to be described as an autoregressive moving average (ARMA) random process (Hayes 1996). The AR parameters may be estimated from compliance measurements as described in Bechtel et al. 2006 and 2007, or by other means. At least to begin, the number of AR parameters used may be very small, perhaps just one, which statistically relates compliance values in adjacent length increments.

Overview of the method for estimating local *E* by using a Kalman filter

An ARMA process can be modeled as the output of a linear dynamic system and represented in state-space format (Schwarz and Friedland 1965, Ogata 1987, Papoulis 1991) where the state vector components, i.e., the state variables $s_i(k)$ of **Figure 8**, correspond with local compliance values within the bending span. In this format, the system model is ready for application of a Kalman filter (Kalman 1960).[3]

The Kalman filter uses a previous state vector estimate, its covariance matrix and a new compliance measurement to compute an updated state vector estimate along with its covariance matrix. By this means the local compliance estimates and their variances are obtained because local compliances are in correspondence with the state variables. At each stage, the Kalman estimation process may be organized into two steps, prediction and then correction. Before a measurement, predictions of the state vector and the measurement are made based on the present state vector estimate and the ARMA model. After a measurement, the difference between the actual measurement and the predicted measurement is used to correct the state vector estimate. These iterative steps are repeated until each measurement in the sequence of bending measurements of the beam has been processed. Whenever, a local compliance value no longer will contribute to a measurement, i.e., when it is about to leave the bending span or when all compliance measurements have been used, the most recent Kalman estimate of the corresponding state vector component is taken as the estimate of that local compliance value.

While a sequence of compliance measurements C_m is formed simply as the reciprocals of their respective modulus of elasticity measurements E_m, local E estimates are not obtained from local C estimates in quite the same way. Each local C estimate C^* is established by the Kalman filter as the mean value of a distribution that has a variance V_C. It is not true that the mean value E^* of a corresponding E distribution is the reciprocal of C^*. If the variance V_C is small, the error may not be large by taking the reciprocal in this way. However, it is better to make a correction based on the *coefficient of variation* (COV_C) of the C distribution:

$$COV_C = \frac{\sqrt{V_C}}{C^*} \qquad [6]$$

After a first order correction, the local E estimate and its coefficient of variation are (Papoulis 1991):

[2] It is not required that the number of autoregression parameters equals the number p of increments in the bending span subdivision. In the examples to follow only one autoregression parameter is used. Also, the number of autoregression parameters can exceed the number p. In that case the AR part (the upper part) of Figure 8 would extend further to the left. However, obtaining information to adequately determine more than a small number of autoregression coefficients may be difficult.

[3] Kalman's seminal 1960 work has found numerous applications. An excellent text (Kailath et al. 2000) puts Kalman's paper in perspective with other topics in estimation theory. Another recent text (Eubank 2006) is useful. The present application is a little unusual in its identification of the state vector with local compliance values.

$$E^* \cong \frac{1}{C^*}\left[1 + COV_C^2\right]$$
$$COV_E \cong COV_C \frac{1}{\left[1 + COV_C^2\right]} \qquad [7]$$

Additional details of the estimation method may be found in (Bechtel et al. 2006 and 2007).

Advantages of the method

1. Fourier transforms are not required, which eliminates the problems of end effects and noise amplification.
2. The method is iterative and computationally efficient. Each result is used as input in obtaining the next. Local estimates may be obtained for the leading end of a wood beam while the trailing end is still being tested in a machine.
3. The method is optimal in a least squares sense against the assumptions used.
4. Tests show feasibility of real-time data-processing in the production line with microcomputer technology and operating with a 55.6 mm sampling interval. Tests indicate that sampling every 55.6 mm is sufficient, which corresponds to a subdivision of wood beams into 55.6 mm length increments. Local C and E estimates are associated with each increment. It is feasible to preprocess the 13.9 mm measurement data from high-speed MSR production equipment with a decimation filtering step (Oppenheim and Schafer 1989), thereby using these data for measurement noise reduction while increasing the sample period to 55.6 mm. Real-time processing is likely not feasible using the 13.9 mm data directly without the decimation step because this finer subdivision greatly increases computational requirements. Real-time processing with a 27.8 mm sampling interval (half of 55.6 mm) may be feasible because computing power has increased since the tests were performed.
5. *A priori* information about statistical properties of a wood beam population can be included. Autoregressive parameters used in the model may be dependent on the populations tested, and these may be first estimated and then refined from compliance measurements as part of the production process.
6. The variance of each estimate is given. Thus, the estimates are obtained with a measure of estimation quality.
7. Estimates are obtained out to the ends of each tested beam, although the estimation quality near beam ends is low.
8. The method allows different bending spans and different span functions to be used as a wood beam passes through a bending machine. This is important in high-speed production-line machines where the bending span changes during the measurement of each beam.
9. The method framework can be expanded to include additional measurements, thereby using a sequence of vector measurements instead of the sequence of scalar measurements presented here for estimating beam properties.

Results

The following results use the ARMA model of **Figure 8**, but all AR coefficients are set to zero except for $a_1 = P$, where

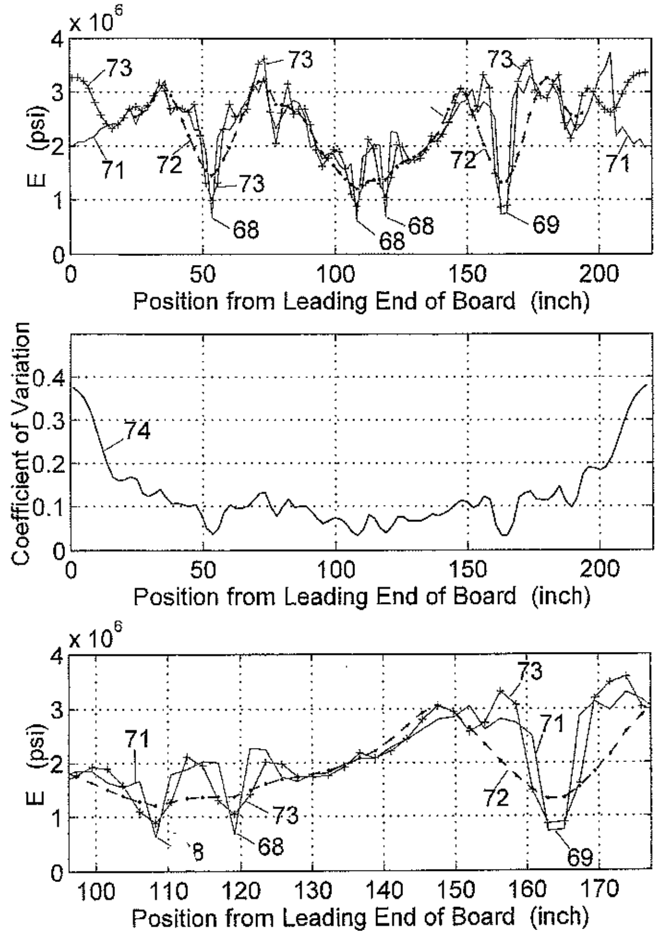

Figure 9. — Results from a simulated wood beam having generated local E *function, curve* ***71****. Simulated measurements* E_m*, curve* ***72****, were obtained by convolving reciprocals of* ***71*** *with the span functions of* ***Figure 4*** *in the appropriate sequence. Kalman estimates of local* E *comprise curve* ***73****. The lower window is expanded from the upper so that detail is more easily seen. Curve* ***74*** *in the central window shows* COV_E *for the local* E *estimates.*

P is a correlation coefficient for the compliance values between adjacent length increments.

Simulated data

Figure 9 illustrates results using a simulation process to generate local modulus of elasticity of a wood beam. A correlation value of P = 0.97 was used in the generation of local compliance data and reciprocals taken to yield curve **71**. Additionally, low points one sample period wide were placed at the locations marked **68**, and two sample periods wide at the location marked **69**. The simulated local compliance data of curve **71** were convolved with the sequence of span functions of **Figure 4** to give simulated measured compliance data, thereby simulating passing a wood beam with the simulated local values through a production-line machine having the bending support arrangement of **Figure 3**. Taking reciprocals yielded the simulated measured E_m of curve **72**. Note that these data do not extend to the ends of the simulated beam because there are not as many measurements as there are increments in the beam subdivision. Bending measurements cannot be taken out to the beam ends because of the necessity

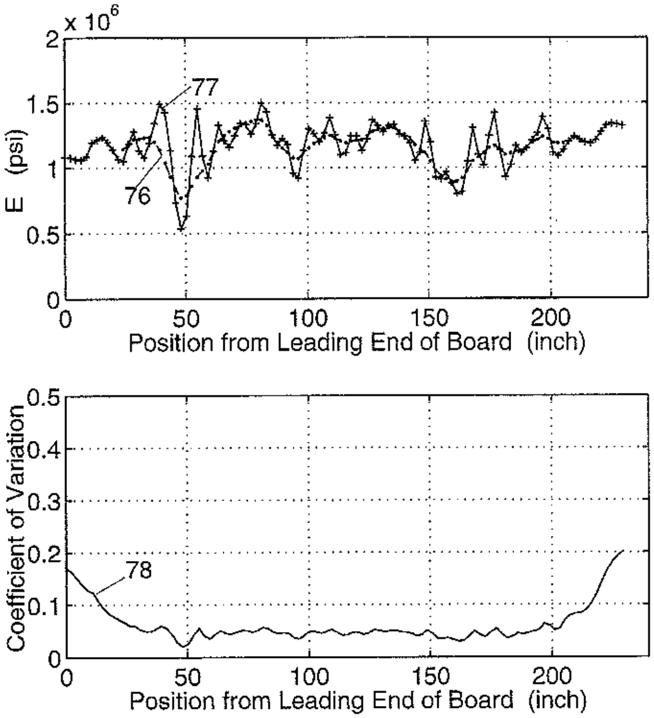

Figure 10. — Shown are measured E_m*, curve* ***76****, from a 38 mm by 140 mm by 6.1 m (2-in. by 6-in. by 20-ft) wood beam of Canadian Spruce-Pine-Fir; Kalman estimated local* E*, curve* ***77****; and* COV_E*, curve* ***78****.*

of completing the bending spans. The "measured" E_m data were processed by the methods described, but with P = 0.90 in the model for use with the Kalman filter, to obtain the local E function of curve **73**. The introduced low points provide justification for the lower assumed correlation coefficient than used to generate the local compliance data. **Figure 9c** is an expanded window from **Figure 9a** to better see detail near the local E minima. **Figure 9b** shows the coefficients of variation for the local E estimates. The estimated local E follows the simulated local E more closely than the "measured" E_m; however, from **Figure 9a**, it is clear that estimation is not good near the ends of the piece as is also clear from **Figure 9b**, which shows large *COV* near the ends.

Real data

Figure 10 illustrates real measured data from a piece of dimension lumber 38 mm by 140 mm by 6.1 m (1.5 inch by 5.5 inch by 20 ft) from a spruce-pine-fir population in central British Columbia, Canada. **Figure 10a** illustrates the measured E_m as curve **76**. The computed local E function, curve **77**, was obtained with a correlation coefficient of P = 0.90 in the AR model for local compliance.

No comparison with true local E is possible because it is unknown. However, it seems likely that estimated local E with a minimum of about 0.55E6 psi (3.8E9 Pa) just before the 50-inch mark might be more useful in an accurate categorization of structural grade than measured E_m with a minimum of about 0.80E6 psi (5.5E9 Pa).

Initialization parameters and conditions for the estimation process are discussed more fully in the literature (Bechtel et al. 2006 and 2007). Many other experiments were made with different combinations of parameters. If the correlation coefficient is set very close to one, so that adjacent local compliance values are assumed highly correlated, then the computed local E tracks the measured E_m curve very closely (not illustrated), but without the measurement noise that is apparent on measured E_m data sets. This provides a practical lead-in to use of the method in the production line. While the method is undergoing testing and improvement to better estimate local E and other structural properties, it can be used to reduce noise and likely increase grading accuracy without affecting other aspects of an MSR sorting and quality control program.

Summary and conclusions

A method was developed to optimally estimate local modulus of elasticity at MSR lumber production speeds. A result was observed that will have immediate benefit in the MSR grading process. Working with a correlation coefficient artificially close to one, the estimated local modulus of elasticity was observed to track very closely with the measured modulus of elasticity, but without the noise that can occur on the measured signal. Because of the very high throughput of MSR machinery, reducing measurement noise alone may improve the grading accuracy enough to pay for further research required to fully achieve our second objective. Commercial implementation will involve primarily additional software.

Additional research required to fully achieve the second objective

While operating with a correlation coefficient artificially close to one and accepted quality control procedures, the less noisy signal should allow machine threshold adjustments for higher grade yields. Further yield benefits likely under the present North American MSR grading process may be tested by experimenting with small reductions in the correlation coefficient while adjusting machine thresholds to maintain process control.

Our method uses an autoregressive model to specify statistical structure among local compliance values and a moving average model to define compliance measurement. Improvements may be possible by including other models of specifying statistical structure for local properties of interest as well as local compliance. Some steps have been taken in this direction for local increments of 610 mm or longer (Kline et al. 1986, Taylor and Bender 1989 and 1991, Richburg et al. 1991, Hernandez et al. 1992, Richburg and Bender 1992, Taylor et al. 1992, Lam et al. 1993). Although we are concerned with local increments about one-tenth or less of the lengths used in these references, the modeling ideas of these cited references provide interesting background material.

Additional measurements that can be identified as weighted combinations of local compliance and/or other local properties may be implemented as components of a vector measurement sequence. Then instead of a sequence of scalar measurements, a sequence of vector measurements can be input to a Kalman filter. Possible measurements include density (Schajer 2001), grain angle (Bechtel and Allen 1990), and dielectric properties (Bechtel et al. 1995 and 1997). In the 1990 reference cited, a "tracks" method was proposed and tested. The tracks method used measured E_m and grain angle to develop an estimator for tensile strength and achieved an r^2 = 0.91 for a small 24 piece sample. While it is unknown if our estimated local E used as input would have produced a better result, it was conjectured then that the excellent results achieved may have been partially due to the limited span lengths over which testing was done.

Literature cited

Bechtel, F.K. 1985. Beam stiffness as a function of pointwise E, with application to machine stress rating. *In*: Proc. Int'l Symp. on Forest Products Res. CSIR. Pretoria, South Africa.

__________. 2007. Estimating local compliance in a beam from bending measurements—Part I: Computing "Span Function." Wood and Fiber Sci. 39(2).

__________ and J.R. Allen. 1985. A noise reducing method for deconvolution. Unpublished. Metriguard Inc. Pullman, WA.

__________ and __________. 1990. Non-destructive testing methods for lumber. U.S. Patent No. 4,926,350.

__________, __________, and D.A. Uskoski. 1995. Dielectric Sensor. U.S. Patent No. 5,394,097.

__________, __________, and __________. 1997. Dielectric Sensor Apparatus. U.S. Patent No. 5,654,643.

__________, C.S. Hsu, and T.C. Hanshaw. 2006. Method for estimating compliance at points along a beam from bending measurements. U.S. Patent No. 7,047,156.

__________, __________, and __________. 2007. Estimating local compliance in a beam from bending measurements-- Part II: Optimal estimation of local compliance. Wood and Fiber Sci. 39(2).

__________, R.K. Byers, J.D. Logan, J.R. Allen, M.G. Strevy, and D.A. Uskoski. 1996. Apparatus for testing lumber stiffness. U.S. Patent No. 5,503,024.

Eubank, R.L. 2006. A Kalman Filter Primer. Chapman & Hall/CRC. New York. 186 pp.

Foschi, R.O. 1987. A procedure for the determination of localized modulus of elasticity. Holz als Roh- und Werkstoff 45:257-260.

Guillemin, E.A. 1949. Mathematics of Circuit Analysis. MIT Press. Cambridge, MA. 590 pp.

Hayes, M.H. 1996. Statistical Digital Signal Processing and Modeling. Wiley and Sons. New York. 608 pp.

Hernandez, R., D.A. Bender, B.A. Richburg, and K.S. Kline. 1992. Probabilistic modeling of glued-laminated timber beams. Wood and Fiber Sci. 23(3):294-306.

Higdon, A., E.H. Ohlsen, and W.B. Stiles. 1960. Mechanics of Materials. Wiley and Sons. New York. 502 pp.

Kailath, T., A.H. Sayed, and B. Hassibi. 2000. Linear Estimation. Prentice-Hall. Upper Saddle River, NJ. 854 pp.

Kalman, R.E. 1960. A new approach to linear filtering and prediction problems. Trans. ASME J. Basic Engineering. Series D. 82D:35-45.

Kass, A.J. 1975. Middle ordinate method measures stiffness variation within pieces of lumber. Forest Prod. J. 25(3):33-41.

Kline, D.E., F.E. Woeste, and B.A. Bendtsen. 1986. Stochastic model for modulus of elasticity of lumber. Wood and Fiber Sci. 18(2):228-238.

Lam, F., R.O. Foschi, J.D. Barrett, and Q.Y. He. 1993. Modified algorithm to determine localized modulus of elasticity of lumber. Wood Sci. and Tech. 27:81-94.

Ogata, K. 1987. Discrete Time Control Systems. Prentice-Hall. Englewood Cliffs, NJ. 994 pp.

Oppenheim, A.V. and R.W. Schafer. 1989. Discrete Signal Processing. Prentice-Hall. Englewood Cliffs, NJ. 879 pp.

Orosz, I. 1976. Relationship between apparent modulus of elasticity, gage length, and tensile strength of lumber. Wood Sci. and Tech. 10: 273-291.

Papoulis, A. 1991. Probability, Random Variables, and Stochastic Processes. McGraw-Hill. New York. 666 pp.

Pope, D.J. and F.W. Matthews. 1995. A comparison of deconvolution techniques to improve MOR estimation from stress grading machine output. Wood Sci. and Tech. 29:431-439.

Richburg, B.A. and D.A. Bender. 1992. Localized tensile strength and modulus of elasticity of E-rated laminating grades of lumber. Wood and Fiber Sci. 24(2):225-232.

__________, R. Hernandez, B.J. Hill, and D.A. Bender. 1991. Machine stress grading for determining localized lumber properties. Pap. No. 91-4542. Inter. Winter Meeting of the ASAE. Chicago, IL.

Schajer, G.S. 2001. Lumber strength grading using x-ray scanning. Forest Prod. J. 51(1):43:50.

Schwarz, R.J. and B. Friedland. 1965. Linear Systems. McGraw-Hill. New York. 521 pp.

Taylor, S.E. and D.A. Bender. 1989. A method for simulating multiple correlated lumber properties. Forest Prod. J. 39(7/8):71-74.

__________ and __________. 1991. Stochastic model for localized tensile strength and modulus of elasticity in lumber. Wood and Fiber Sci. 23(4):501-519.

__________, __________, D.E. Kline, and K.S. Kline. 1992. Comparing length effect models for lumber tensile strength. Forest Prod. J. 42(2): 23-30.